COMPDYN 2013
4th ECCOMAS Thematic Conference on
Computational Methods in Structural Dynamics and Earthquake Engineering
M. Papadrakakis, V. Papadopoulos, V. Plevris (eds.)
Kos Island, Greece, 12–14 June 2013

DESIGN AND ASSESSMENT OF STEEL AND STEEL-CONCRETE COMPOSITE STRUCTURES: EFFICACY OF EN1998 DESIGN PROCEDURE.

A. Braconi[1], S. Caprili[2], H. Degee[3], M. Guendel[4], M. Hjaij[5], B. Hoffmeister[4], S. Karmanos[6], V. Rinaldi[7], W. Salvatore[2]

[1] RIVA FIRE S.p.A., Viale Certosa, Milano, Italy
aurelio.braconi@gmail.com

[2] Department of Civil and Industrial Engineering University of Pisa, Italy
silvia.caprili@ing.unipi.it, walter@ing.unipi.it

[3] Département ArGEnCo, Universitè de Liege, Belgique
h.degee@ulg.ac.be

[4] RWTH Aachen University, Institut für Stahlbau, Aachen, Germany
guendel@stb.rwth-aachen.de, hoff@stb.rwth-aachen.de

[5] Institut National des Sciences Appliquées de Rennes, France
Mohammed.Hjiaj@insa-rennes.fr

[6] University of Thessaly, Volos, Greece
skara@mie.uth.gr

[7] Arcelor Mittal S.A.
valerie.rinaldi@arcelormittal.com

Keywords: Behaviour factor, Incremental Dynamic Analysis, Pushover analysis

Abstract. *Design codes for seismic constructions allow the realization of structures able to dissipate energy through cyclic plastic deformations localized in specific zones, selected to involve the largest number of structural elements. The capacity design approach requires an opportune selection of the design forces and an accurate definition of structural details in the plastic hinges. The structural elements in which plastic hinges are located are over-sized with respect to the seismic actions obtained by the use of the design spectrum, while the elements that shall remain elastic are over-sized with respect to dissipative elements. The capacity design methodology requires an accurate control of the localization of plastic hinges, strongly influenced by the actual mechanical properties of materials. In the present work, developed inside the research project OPUS, different case studies were designed according to Eurocodes and subjected to a deep structural analysis, aiming to evaluate the effective allowable ductility (behaviour factor) with respect to what imposed during the design phase.*

1 INTRODUCTION

Design codes for seismic constructions nowadays allow to exploit plastic resources by realizing ductile structures able to dissipate energy by means of cyclic plastic deformations localized in the suitably chosen dissipative zones. Plastic deformations have to be located within the structures in such a way to guarantee the involvement of the largest number of structural elements. The larger is the number of the plastic hinges, the larger is the attainable global ductility and the smaller is the deformation demand at local level.

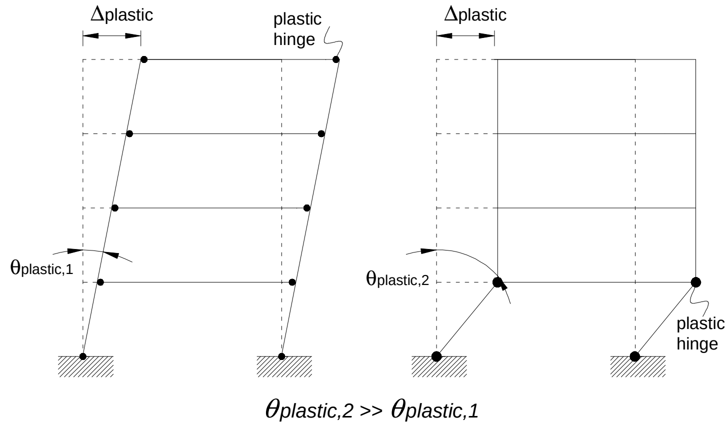

Figure 1: Global ductility vs. local rotation demand for moment resisting frames.

The design of plastic hinges in desired elements and the development of an efficient energetic dissipation, without any significant decrease in terms of resistance or stiffness, are obtained through a proper design methodology called *capacity design* and an accurate definition of structural details of elements, joints and connections. Obviously, the choice of dissipative elements depends on the structural typology; for steel structures, the most diffused are Moment Resisting Frames (MRF), Concentrically Braced Frames (CBF) and Eccentrically Braced Frames (EBF).

In multi-storey buildings, for example, to allow the development of the largest number of plastic hinges and to dissipate as much as possible seismic energy, the condition $\sum M_{Rc} \geq 1.3 \times \sum M_{Rb}$ [1] has to be checked in correspondence of each beam-to-column joint of the structure, being ΣM_{Rc} and ΣM_{Rb} the sums of the design values of the moment resistance of columns and beams, respectively, framing at a joint (figure 2). This condition aims at avoiding the formation of poor dissipative mechanisms as soft-storey, furnishing to the column sufficient overstrength with respect to the beams. The 1.3 factor, in particular, takes into account possible overstrength phenomena of materials used in beams with respect to the ones adopted for columns.

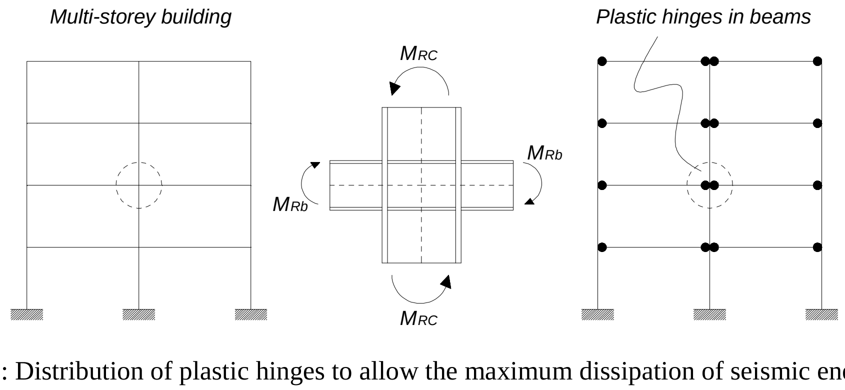

Figure 2: Distribution of plastic hinges to allow the maximum dissipation of seismic energy.

In the modal analysis procedure, commonly used in the engineering practice, the possibility to exploit plastic resources is translated in lower values of design seismic actions. To obtain the design spectrum, the elastic response one is divided by a reduction factor, summarizing the parameters that govern the structural response, the available inelastic resources and the sensibility to the second-order effects.

The aforementioned reduction factor is already introduced by several modern standards such as Eurocode 8 [1], in which it is identified as the behavior factor “q”, or the US standards, Uniform Building Code, UBC [2] NEHRP provisions [3], American Seismic Provisions for Structural Steel Buildings [4], in which the reduction factor “R” is defined. The larger the reduction factor is, the larger shall be the structural ductility and the lower can be the seismic design actions. In such a way it seems possible to obtain systematically structural solutions characterized by a reduced overall weight.

However, the exploitation of the plastic capacity can be limited by other criteria adopted in the design process: for example, in the assessment at serviceability limit state, the limitation of second order effects as well as the assessments of limit states associated to static load combinations shall be considered. The fulfilment of such conditions can limit the benefits of ductile design, leading to a structure whose seismic response can be far from the one supposed at design stage. The structural elements in correspondence of dissipative zones are over-dimensioned with respect to the seismic actions obtained by the design spectrum so that, in practice, only a small percentage of ductile resources will be exploited. At the same time, as the capacity design rules are applied, the protected elastic elements are further over-dimensioned with respect to dissipative elements [5, 6].

Moreover, according to previous concepts, the seismic ductile design foresees an accurate control of plastic hinge’s formation that mainly depends on the distribution of plastic resistances of structural elements. It is so clear that the *capacity design* method strongly depends on the actual mechanical properties of materials.

On the other hand, European production standards [7] do not provide adequate limitations on mechanical material properties for steel products either there is not a good agreement among provisions of different standards. For these reasons, the adoption of aforementioned design approaches is allowed by Eurocode 8 [1], for steel and composite steel-concrete structures, on the conditions that adequate safety factors are introduced and that actual values of the mechanical properties do not modify the location of plastic hinges. These conditions limit the adoption in design practice of the steel and steel-concrete composite structures, potentially a very interesting option in seismic zone because of the intrinsic ductility and dissipative capacity of the steel.

Eurocode 8, in particular, imposes additional checks on material properties in dissipative zones as, for example, in steel members where the yielding stress shall be upper limited by the overstrength coefficient, γ_{OV} fixed equal to 1.25 (1.25 times the nominal yielding value f_y).

Some first evaluations on seismic reliability of steel structures taking into account variability of steel properties were executed on concentrically braced frames [8], and eccentrically braced frames [9] but a well comprehensive study, aiming at clarifying aforementioned open problems, is still missing.

The OPUS research project, *Optimizing the seismic Performance of steel and steel-composite concrete strUctures by Standardizing material quality control*, funded by European Commission through Research Fund for Coal and Steel, contract RFCR-CT-2007-00039 [10], aimed at assessing the influence of material properties’ scattering on final structural performance of steel and steel concrete composite structures designed in earthquake-prone areas. In particular, in the framework of this project, a representative set of case studies, including MRFs, EBFs and CBFs, was designed according to the Eurocode design provisions and afterwards subjected to a deep analysis of their structural performance. A suitably developed probabilistic procedure then allowed to estimate the failure probability associated to all relevant collapse modes previously identified.

In the present paper the main results obtained by aforementioned performance analysis of the case studies are illustrated and discussed while [11] includes the main results on influence of material properties' scattering on final structural performance.

The assessment of seismic performance of all structures was executed developing plain non-linear models of the main resisting frames: about 40 models were elaborated and calibrated through a complete benchmarking process devoted to the simulations of three structural typologies. The models were analyzed employing Push-Over analysis (PO) and Incremental Dynamic Analysis (IDA) in order to characterize the structural behavior of case studies and to individuate the relevant collapse modalities.

The analysis on structural case studies was further pushed in more refined details in order to assess the real behavior factor (q) of all models and to individuate the level of Peak Ground Acceleration (PGA) able to activate the collapse modes previously identified. In particular, IDA technique was applied and, once identified the PGA able to activate relevant collapse modes, the Ballio-Setti procedure [12, 13] was used to determine the q factor.

Moreover, the Ballio-Setti procedure was slightly modified for taking into account the discrepancy at first mode frequency between the target spectra and real spectra of earthquake time-histories. Such procedure allowed to compare for each considered case-study actual value of q-factor with the one used in the design process.

2 DESIGN OF THE CASE STUDIES

A fully representative set of case studies, including MRFs, CBFs and EBFs was designed according to Eurocode prescriptions: the geometries and the morphologies were suitably chosen in order to house offices, car parks, industrial storages, electrical power plants or ware house/light industrial activities; some examples of the designed buildings are reported in the figure 3. Two levels of seismic actions were selected in order to represent low and high seismic hazard areas; the static loads were chosen on the basis of housed activities according to EN1991 [14] and the wind action was selected fixing a unique parameters for all structures. In the table 1 all the information related to use category, live loads, environmental loads (snow, wind and earthquake) are presented, while geometry, chosen resisting systems for vertical and horizontal loads and floor system scheme are listed in the table 2.

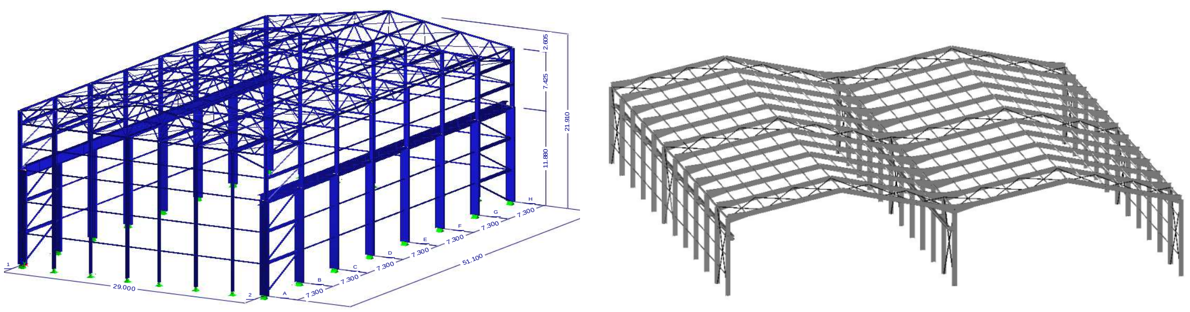

a) b)

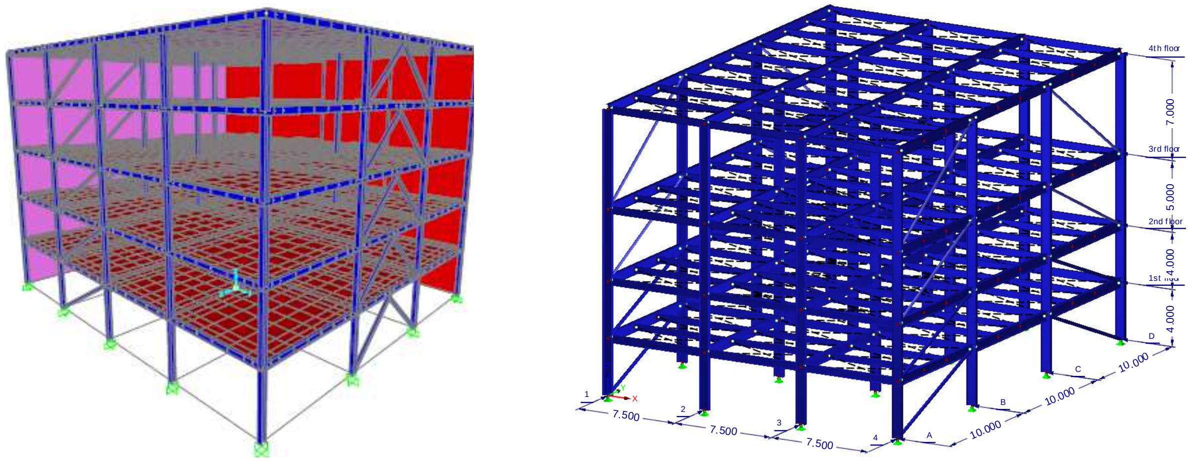

c) d)

Figure 3: a) Industrial building for electrical power plant activities; b) industrial building for warehouse/light activities; c) EBF and CBF configurations for offices; d) MRF and CBF configurations for industrial storage

Building n°	Building type	Material	Live Load kN/m²	Snow kN/m²	Wind kN/m² (m/s)	Seismic action PGA [g]
1	Office	Steel	3,00	0,85	0,39	0,10
2	Office	Steel	3,00	0,85	0,39	0,10
3	Office	Steel	3,00	1,00	1,10	0,25
4	Office	Steel	3,00	1,00	1,10	0,15
5	Office	Steel	3,00	1,40	(30 m/s)	0,25
6	Office	Composite beams/ Steel columns	3,00	1,11	1,40	0,10
7	Office	Composite beams and columns	3,00	1,11	1,40	0,10
8	Office	Composite beams/ Steel columns	3,00	1,11	1,40	0,25
9	Office	Composite beams and columns	3,00	1,11	1,40	0,25
10	Office	Composite beams/ Steel columns	3,00	1,11	1,40	0,10
11	Office	Composite beams and columns	3,00	1,11	1,40	0,25
12	Industrial	Steel	5,00	1,40	(30 m/s)	0,25
13	Industrial	Steel	Crane load (10 tons)	1,40	(30 m/s)	0,25
14	Industrial	Steel	Crane load (370+140 tons)	0,85	0,39	0,25
15	Industrial	Steel	5,00 kN/m² + add. dead loads (6,8 kN/m²)	0,85	0,39	0,10
16	Car Park	Steel	2,50	1,00	1,10	0,25

Table 1:Structural typologies and design loads used for case studies.

Building ID	N°of storeys	X – direction				Y – direction			
		Resisting System	Span [m]	Secondary beam	Storey height [m]	Resisting system	Span [m]	Secondary beam	Storey height [m]
1	5	MRF	3x7m	Yes	3,5	CBF	6x6m	No	3,5
2	5	CBF	3x7m	Yes	3,5	CBF	6x6m	No	3,5
3	5	EBF shear	3x7m	No	3,5	EBF shear	4x6m	Yes	3,5
4	5	EBF bending	3x7m	No	3,5	EBF bending	4x6m	Yes	3,5
5	5	MRF	3x7,5m	Yes	3,5	CBF	4x6m	Yes	3,5
6	5	MRF	3x7m	Yes	3,5	Not designed	4x6m	No	3,5
7	5	MRF	3x7m	Yes	3,5	Not designed	4x6m	No	3,5
8	5	MRF	3x7m	Yes	3,5	Not designed	4x6m	No	3,5
9	5	MRF	3x7m	Yes	3,5	Not designed	4x6m	No	3,5
10	5	EBF shear	3x7m	No	3,5	CBF	4x6m	No	3,5
11	5	EBF shear	3x7m	No	3,5	CBF	4x6m	No	3,5
12	4	MRF	3x7,5m	Yes	4+4+5+7	CBF	3x10m	No	4+4+5+7
13	1	MRF	2x25m	Yes (purlins)	10,5	CBF	12x6m	Yes (purlins)	10,5
14	1	MRF truss girder	1x29m	No	21,9	CBF	7,30m	No	17,6
15	4	MRF	3x7,5m	No	4+4+5+7	CBF	3x10m	Yes	4 +4 + 5+7
16	2	EBF shear	5x8m 2x10m	No	4+4	EBF shear	6x10.5m	Yes	4+4

Table 2: Structural and geometrical characteristics of designed case studies.

The design procedure followed actual European and international standards [1, 14, 15, 16, 17]; in particular, the design process was repeated for all structures adopting different strategies or techniques, in order to optimize the cross sections' size and to avoid the over-sizing of structural members, a relevant aspect especially for low seismicity areas in which seismic forces can be lower than wind ones. The optimal design was not reached in all cases because of design procedures, checks and limitations imposed by Eurocodes.

In the case of MRFs, it was noted that the contemporary assessment of design checks both for static and seismic combinations obliged to over-size beams respect to seismic strength requirements. In addition, capacity design approach, beam-to-column resistance hierarchy, drift limitations and sensitivity to second order effects, following respectively equations (1), (2), (3) and (4), strongly conditioned the final sizing of the elements:

$$E_i^{c.d.} = E_i^{gravity} + 1.1 \cdot \gamma_{OV} \cdot \min(\Omega_j) \cdot E_i^{seismic} \tag{1}$$

$$\sum M_{Rd,PL}^{column} \geq 1.3 \cdot \sum M_{Rd,PL}^{beam} \tag{2}$$

$$\nu \cdot q_d \cdot d_e = \nu \cdot d_r \leq d_{\lim it} \tag{3}$$

$$\vartheta = \frac{P_{tot} \cdot d_r}{V_{tot} \cdot h} \leq \beta \tag{4}$$

where E_i is the solicitation acting on the i-th member, γ_{ov} is the material over-strength (equal to 1.25), $M_{Rd,PL}$ is the design resistant bending moment, d_e is the elastic drift coming from analyses, q_d is the displacement behaviour factor taken equal to q, P_{tot} and V_{tot} are respectively total vertical actions and horizontal action on the i-th floor.

Ω factor represents the structural over-strength, i.e. how higher is the resistance of the more solicited dissipative member respect to the maximum level of solicitations in the seismic combination, expressed by equation (5):

$$\Omega_i = \alpha \cdot \frac{R_{d,i}}{E_{i,dissipative}^{seismic}} \tag{5}$$

where α coefficient is equal to 1 for MRFs and CBFs and 1.5 for EBFs.

The over-sizing of dissipative members and the adoption of limitations for interstorey drift ratio notably increased the size of columns and of beams leading, at the end of the design process, to structures with a large amount of strength and ductility resources, higher than the ones effectively required by seismic loads.

In order to cope with these problems, in the case of MRFs it was followed an appropriate design process devoted to the selection of an optimized behaviour factor, harmonized with strength requirements coming from static load combinations. According to this procedure, in many cases, it was found more convenient to design structural configurations adopting medium ductility behaviour rather than high ductility behaviour both in high and low seismicity areas.

In the case of EBF configurations (buildings 3, 4 and 16), a similar problem for sizing seismic links was revealed, since the interaction between static and seismic combinations played an important influence and obliged to over-size seismic link sections; in addition, the control of links over-sizing inside EBF configuration was completed checking that difference between Ω_i of links was not more than 25% (table 4):

$$\frac{\Omega_{\max}}{\Omega_{\min}} \leq 1.25 \tag{6}$$

In buildings n°3 and 4, characterized by a similar geometrical scheme but designed for different levels of PGA and with a different behaviour of link elements (table 2), in order to reduce the over-strength influence on the final design, a suitable technical solution of the floor system was used in order to decuple static effects from seismic effects on the seismic links: beams contained seismic links were coupled with other beams (i.e. beam duplication) devoted to carry vertical loads only. It was so possible to optimize some structural solutions to an utilization ratio of the links (e.g. solicitation/resistance, S/R) equal to 1 arriving so to an over-strength coefficient Ω equal to 1.5. This, anyway, produced an increment of bracing sections. As for the case of MRFs, the design of EBFs was strongly influenced by second order effects and by the respect of drift limitation: as an example, the sizing of braces in frame 3x (building n°3, frame in xz plane) was determined in relation to the satisfaction of the limitation of the maximum drift limit equal to 0.05%, leading to an oversizing of bracing elements; in building 4, on the other side, the most critical condition imposed in the desing was the fulfilment of buckling in members in compression, in which, consequently, the ratio between solicitation and strenght was nearly about 1 (optimization in the design of braces).

Concerning CBF solutions, the design process proposed by EN1998-1 [1] obliged to perform several repetitive designing in order to fulfil problems related to slenderness ratio:

$$1.3 \leq \lambda \leq 2.0 \tag{7}$$

and the assessment of equations (1), (3) and (4).

Only in some cases the optimization was reached arriving to a solicitation/strength ratio near to 1; for other solutions, different steel qualities were adopted for steel bracings at different floor levels in order to optimize design checks and to satisfy all the prescriptions for seismic design (tables 4 and 6).

Obviously, the adoption of several different braces' or beams' sections, different steel grades for braced configurations and the selection of behaviour factors for MRF optimized solutions are not commonly adopted in the current engineering design practice; as a consequence, it can be argued that the design procedure proposed by EN1998-1 [1], without a complete and long conceptual preliminary phase, leads to structures with performance rather higher than the ones strictly required by seismic load combination.

What already presented confirms that EN1998-1 design procedure [1] generally allows the realization of safe structures, evidencing, at the same time, that the impossibility of reaching a full optimized structural solution represents a limit that can endanger the competitiveness of these structural typologies.

ID	*Structural Typology*		*Material*	*Floor*	*Beams*		*Columns*	*Bracing system*	
	x-dir	*y-dir*			*x- dir*	*y- dir*		*x- dir*	*y- dir*
				1	IPE 400	IPE 500		-	CHS 139.7x12.5
				2	IPE 400	IPE 500		-	CHS 139.7x10.0
1	MRF	CBF	Steel S235	3	IPE 400	IPE 500	HEB 400	-	CHS 139.7x8.0
				4	IPE 400	IPE 500		-	CHS 114.3x8.0
				5	IPE 400	IPE 500		-	CHS 114.3x4.0
12	MRF	CBF	Steel S355	1	HEB 360	HEB 400	HEB 450	-	C273,0×8.0
				2	HEB 360	HEB 400		-	C273,0×8.0
				3	HEB 360	HEB 400		-	C273,0×7.1
				4	HEB 360	HEB 400		-	C273,0×7.1
	MRF	CBF	Steel S460	1	HEB 320	HEB 340	HEB 400	-	C273,0×7.1
				2	HEB 320	HEB 340		-	C273,0×7.1
				3	HEB 320	HEB 340		-	C244,5×7.1
				4	HEB 320	HEB 340		-	C244,5×7.1
13	MRF	CBF	Steel S235	1	IPE 500	IPE 120	HEA 500	-	2L120x120x20
	MRF	CBF	Steel S275	1	IPE 450	IPE 120	HEA 500	-	2L120x120x20
15	MRF	CBF	Steel	1	IPE 550	HEA 700	HEB 700	-	CHS 244.5x8.0
				2	IPE 500	HEA 700		-	CHS 244.5x6.0
				3	IPE 500	HEA 700		-	CHS 193.7x10
				4	IPE 500	HEA 700		-	CHS 193.7x4

ID/System		*Lev.*	*Beams*		*Braces y-dir*		*Col.*
		n°	*x- dir*	*y- dir*	*dissipative*	*non diss.*	
14	Steel beams and columns	1	Truss girder as part of MRFs	Simply supported purlins: HEA200	CHS193.7x8	2HEA240	main col.: HEB1000
		2			CHS193.7x8	2HEA240	

	X dir. MRF with truss girder Y dir. CBF	3	chords: HEA180 diag.: CHS139.7x4	fully rigid connectors HEA140	CHS193.7x8	2HEA240	roof col.: HEA450
		4			*CHS168.3x6.3	2HEA240	
		5			*CHS168.3x6.3	2HEA240	

ID/System		*Lev. n°*	*Beams x- dir*	*Beams y- dir*	*Braces Y dissipative*	*Column x- dir*	*Column y- dir*
5	Steel S355 X-dir: MRF Y-dir: CBF	1	IPE330*/IPE450**	IPE270*/IPE330**	S100x8	1° floor: HEA360* HEA400** HEB300^{+} HEB360^{++}	1° floor: HEA360* HEB300** HEA400^{+} HEB360^{++}
		2	IPE330*/IPE450**	IPE270*/IPE330**	S90x8		
		3	IPE330*/IPE450**	IPE270*/IPE330**	S80x8		
		4	IPE330*/IPE450**	IPE270*/IPE330**	S75x6	HEA360* HEA360** HEB300^{+} HEB360^{++}	HEA360* HEB300** HEA360^{+} HEB360^{++}
		5	IPE300*/IPE450**	IPE330*/IPE400**	S60x4		

Table 3: Steel buildings with MRF and MRF-CBF structure: characteristics of structural elements (more details related to building n°5 are presented in [10]).

ID/System/Floor n°			*Beams x*	*Beams y*	*Col.*	*Braces x- dir*	*Braces y- dir*	*Links x*	*Links y*	*Ωi x*	*Ωi y*
2	CBF Steel	1	IPE 400	IPE 500	HEB 340	CHS139.7x12.5	CHS139.7x12.5	-	-	1.14	1.28
		2				CHS139.7x10	CHS139.7x10	-	-	1.11	1.19
		3				CHS139.7x8	CHS139.7x8	-	-	1.11	1.11
		4				CHS139.7x8	CHS114.3x8	-	-	1.32	1.20
		5				CHS139.7x4	CHS114.3x4	-	-	1.37	1.18
3	EBF Steel S355	1	IPE 500	IPE 360	HEB 300 HEB 320	HEB 220	HEB 280	HEB 200	HEB 200	1.66	2.12
		2				HEB 220	HEB 280	HEB 180	HEB 200	1.54	2.47
		3				HEB 220	HEB 260	HEB 160	HEB 160	1.53	2.00
		4				HEB 200	HEB 260	HEB 140	HEB 140	1.62	2.03
		5				HEB 200	HEB 260	HEB 120	HEB 100	1.86	2.24
4	EBF Steel S355	1	IPE 500	IPE 360	HEB 240 HEB 260	HEB 200	HEB 200	IPE 270	IPE 270	1.68	1.99
		2						IPE 270	IPE 270	1.87	1.74
		3						IPE 240	IPE 240	1.63	1.78
		4						IPE 220	IPE 220	1.66	1.76
		5						IPE 160	IPE 160	1.51	1.61
16	EBF Steel S275	1	-	IPE 600	HEB 240	HEB 280	HEB 260	HEB 320	HEB 300	1.53	1.57
		2	-					HEB 360	HEB 280	1.88	1.91

Table 4: Steel buildings with EBF and CBF structure: characteristics of structural elements.

ID	*Typology*	*Lev. n°*	*Beams (x-direction)*					*Column*
6	Composite beams/ Steel columns X dir: MRF Y dir: not des.	1	Fully rigid IPE 360	Concrete effective width [mm]	EC4	Mid.	1225	HEA 450
		2				End.	875	
		3			Elastic EC8	M^-	700	
		4				M^+	525	
		5			plastic EC8	M^-	1400	
		Materials: S235 – C25/35				M^+	1050	
7	Composite beams/ Composite columns X dir: MRF Y dir: not des.	1	Fully rigid IPE 360	Concrete effective width [mm]	EC4	Mid.	1225	HEA 400 Reinfor. steel $4\Phi 24$ mm
		2				End	875	
		3			Elastic EC8	M^-	700	
		4				M^+	525	
		5			plastic EC8	M^-	1400	
		Materials: S235 – C25/35				M^+	1050	
8	Composite beams/ Steel columns X dir: MRF Y dir: not des.	1	Fully rigid IPE 360	Concrete effective width [mm]	EC4	Mid.	1225	HEA 400
		2				End	875	
		3			Elastic EC8	M^-	700	
		4				M^+	525	
		5			plastic EC8	M^-	1400	
		Materials: S355 – C30/37				M^+	1050	
9	Composite beams/ Composite columns X dir: MRF Y dir: not des.	1	Fully rigid IPE 360	Concrete effective width [mm]	EC4	Mid.	1225	HEA 360 Reinfor. steel 4Φ 24mm
		2				End	875	
		3			Elastic EC8	M^-	700	
		4				M^+	525	
		5			plastic EC8	M^-	1400	
		Materials: S355 – C30/37				M^+	1050	

Table 5: Composite structures with MRF system (no braces).

ID	*Structural system*	*Lev. n°*	*Beams x- dir*	*y- dir*	*Braces Y dissipative*	*non diss.*	*Braces Y dissipative*	*Column*
10	Composite beams/ Steel columns X dir: EBF (shear) Y dir: CBF	1	IPE 270 + slab 0,18 m	IPE 270 + slab 0,18m	HEB 260	HEB 180	UPE 160	HEB 300 strong axis X
		2			HEB 260		UPE 200	
		3			HEB 220		UPE 160	
		4			HEB 200		UPE 120	
		5			HEB 160		UPE 80	
11	Composite beams/ Steel columns X dir: EBF (shear) Y dir: CBF	1	IPE 270 + slab 0,18 m	IPE 270 + slab 0,18m	HEB 450	HEB 240	UPE 180	HEB260 strong axis X (except for ground storey – HEB 280)
		2			HEB 450		UPE 200	
		3			HEB 400		UPE 180	
		4			HEB 340		UPE 140	
		5			HEB 280		UPE 100	

Table 6: Composite structures with bracing systems.

3 DEVELOPMENT OF STRUCTURAL MODELS

The presented case studies were deeply analyzed adopting sophisticated models able to capture all relevant non-linear phenomena at structural and material level. The main aims of the present work consisted in the individuation, for each structure, of the relevant collapse criteria and of the corresponding PGA activation level and, moreover, in the evaluation of the seismic structural performance in terms of behaviour factor q. To these purposes, suitable numerical models were developed.

Given that the numerical simulations were carried out by different partners of OPUS project [10] using different software like Abaqus [21], FineLG [22], Dynacs [23] and OpenSees [24], a calibration process was executed comparing simulated capacities on simple benchmarks. Three different structures (a bracing element, a portal frame and a concentrically braced frame) were modelled and used as calibration case studies: modelling parameters employed for the definition of numerical models of the structures previously design were consequently fixed [10].

The structural behaviour of buildings n° 1, 2, 14 and 15 was investigated by using the finite element program Dynacs [23]. The structures were modelled using bi-dimensional frames with fibre beam elements, with increasing element density in dissipative regions of the MRFs (e.g. column base, beam-column connections). The non-linear material behaviour was considered adopting a bi-linear model with kinematic hardening described by yield stress, tensile stress and ultimate elongation. Braces were modelled using special developed non-linear springs elements, representing the elastic-plastic cyclic behaviour under tension, global buckling under compression and cyclic degradation. The analyses included large deformations to consider the influence of the P-Δ-effect.

Buildings n° 6, 7, 8, 9, 10 and 11 were assessed using the non linear finite element software FineLG [22]. Composite elements were modelled using fibre beam element including a steel and a concrete part. The concrete part was assumed to be a rectangular beam element with width equal to the effective one evaluated according to Eurocode 4. Diagonal members of EBF and CBF structures were modelled using steel beam element directly taking into account the possible lateral buckling under compression. The seismic links in EBF needed to include the yielding in shear, generally not possible with the adoption of classical fibre models: as a consequence, the link elements were modelled by a classical non linear beam element describing properly the bending behaviour, coupled with a non linear spring calibrated versus a shell model and accounting for the shear deformation and yielding, as briefly schematized in the figure 4.

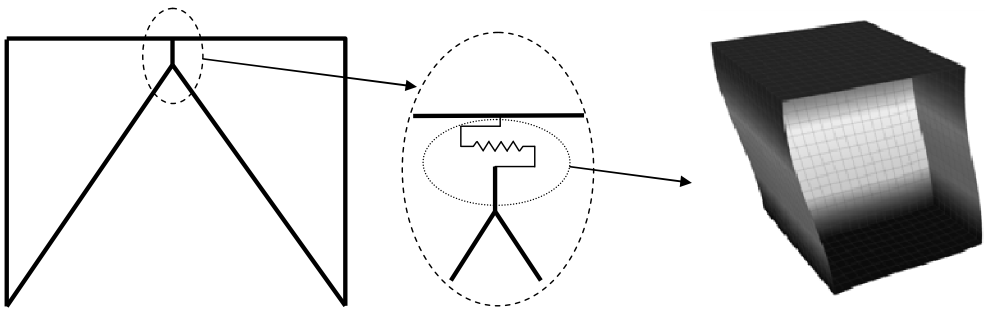

Figure 4: Modelling of the seismic shear link

Buildings n° 5, 12 and 13 were modeled by Abaqus software [22]: beams and columns were modeled using 3-node quadratic beams in plane for MRF and 3-node quadratic beams in space for concentrically braced frames.

Buildings n° 3, 4 and 16 were modeled using the numerical software OpenSees [24]. The dissipative behavior of link elements and the combined effect of shear forces and bending moments were directly taken into account modeling all the elements as fiber section elements (figure 5a). Inelastic fiber elements were used for representing columns, beams without links and short shear links; two elements were used for modeling each long bending link and four elements were employed for each brace. Buckling phenomena of braces were directly taken into account giving an initial imperfection equal to 1/500 of the brace length to the middle point of the brace itself, as represented in figure 5b; a similar imperfection was also assigned to the top of columns in order to include in the analysis P-Δ effect (figure 5b). The value adopted for the imperfection was evaluated from the calibration with literature results.

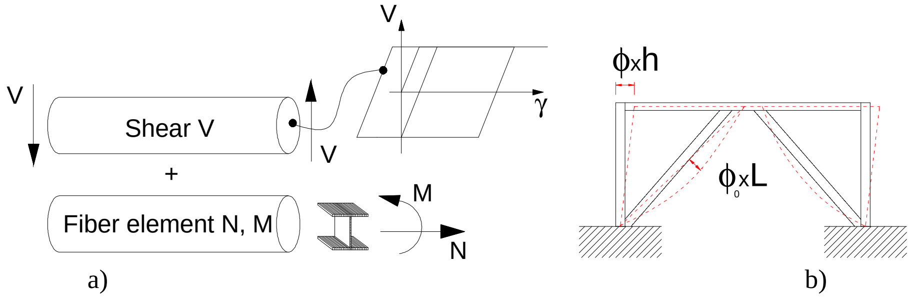

Figure 5: a) General scheme of fiber elements and b) model of imperfections of braces and columns.

For modeling the flexural behavior of steel members (beams, braces and columns), the Menegotto-Pinto law [25], characterized by bilinear elastic-plastic stress-strain curve with kinematic hardening, accurately calibrated in order to agree with literature results, was used (figure 6a); moreover, as regards the force-distortion law used for representing the shear behavior of elements, a bilinear elastic-plastic law with kinematic hardening was used for links (figure 6b).

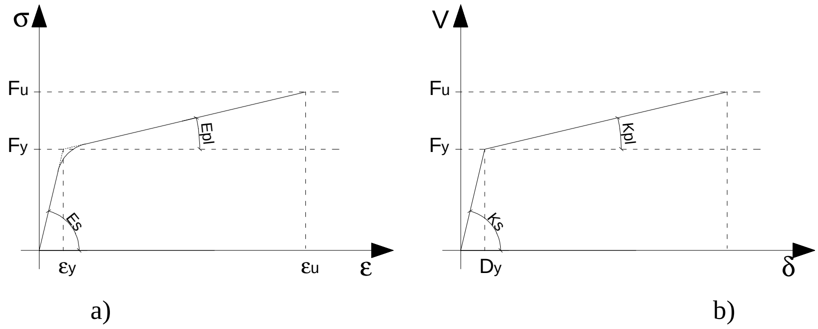

Figure 6: Constitutive law adopted for a) flexural behaviour, b) shear behaviour of dissipative elements.

4 ANALYSIS OF STRUCTURAL PERFORMANCE

4.1 Definition of collapse criteria

Seismic demand levels are usually defined in relation to performance levels as Damage Limitation (DL), Severe Damage (SD) and Near Collapse (NC). The investigations hereafter presented were carried out for the SD performance level, according to EN1998-3 [18] and corresponding to an earthquake hazard level with a medium return period of 475 years.

A crucial point in the assessment of structures using non-linear static and dynamic analysis is the definition of limit states, not exactly defined in European seismic standards. The seismic performance of structures can be evaluated by general deformation criteria (i.e. for example the over-passing of the interstorey drift limit) or local ductility criteria. Furthermore, non seismic-specific verifications as shear capacity, global buckling, and others shall be also carried out.

Global deformation criteria as roof and storey drift defined according to FEMA356 [19] were only used as indicative values. Additionally, maximum connection forces and foundation forces were recorded for further investigations. All verifications were carried out for each structural element with regard to the maximum value obtained during a time history analysis automatically by user-defined subroutines. Only global buckling and lateral torsional buckling were checked manually in the relevant time step.

The limit axial load for the buckling of steel members in compression (columns and braces) was evaluated according to Eurocode 3 with expression (8), and was consequently strongly influenced by the mechanical properties of materials (yielding strength f_y):

$$N_{b,Rd} = \frac{\chi \cdot A \cdot f_y}{\gamma_{M1}} \tag{8}$$

All limit states considered in the case studies with moment-resisting (MRF) and concentrically braced steel frames (CBF) are presented respectively in tables 7 and 8.

For eccentrically braced frames (EBF) one of the most conditioning collapse criteria was obviously the failure of link elements, in which plastic deformation are concentrated according to the design principles. The plastic rotation was calculated as the ratio between the relative vertical displacement (δ) and the link length (e):

$$\frac{v_1 - v_2}{e} = \frac{\delta}{e} = \gamma_{LINK} \tag{9}$$

where for shear short link δ was evaluated as the relative vertical displacement between the two ends of the link (figure 6a) and for long bending links δ referred to the mid length of the element (figure 6b). The limits assumed for EBF are presented in the table 9.

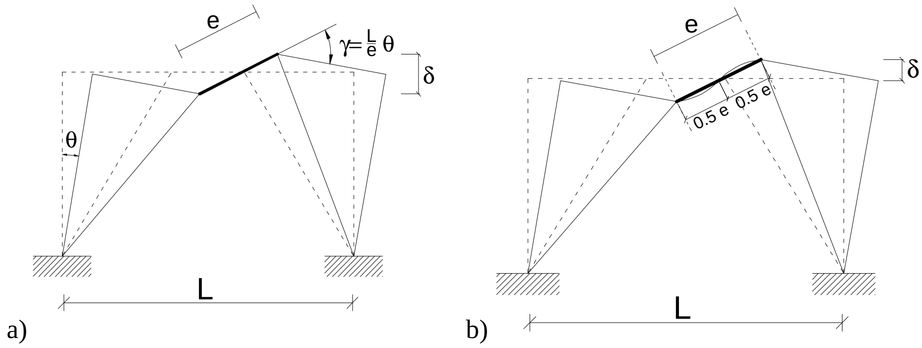

Figure 7: Evaluation of link plastic rotation a) for short shear links, b) for long bending links.

	Type	Reference	Criteria
A	Dynamic instability (Global)	-	Limit
B	Maximum roof drift ratio (Global)	FEMA 356	Indicative
C	Inter-storey drift ratio (Global)	FEMA 356	Indicative
D	Ultimate rotation of plastic hinges (Local) *	EN1998-3	Limit
E	Shear capacity (Local)	EN1993-1	Limit
F	Lateral torsional buckling (Local) **	EN1993-1	Limit
G	Global buckling (Local)	EN1993-1	Limit
H	Joint forces	-	Evaluation
I	Foundation forces	-	Evaluation

Table 7: Failure criteria for buildings with MRF. (*) for axial load ration $0.3 < n \leq 0.5$ linear reduction of rotation capacity in acc. to FEMA356; (**) Lateral torsional buckling of beams is prevented by RC-floor (no composite action)

	Type	Reference Code	Criteria
A	Dynamic instability (Global)	-	Limit
B	Maximum roof drift ratio (Global)	FEMA 356	Indicative
C	Inter-storey drift ratio (Global)	FEMA 356	Indicative
L	Ultimate deformation, tension (Local)	EN1998-3	Limit
M	Ultimate deformation, compression (Local)	EN1998-3	Limit
E	Shear capacity (Local)	EN1993-1	Limit
F	Lateral torsional buckling (Local) **	EN1993-1	Limit
G	Global buckling (Local)	EN1993-1	Limit
H	Joint forces	-	Evaluation
I	Foundation forces	-	Evaluation

Table 8: Failure criteria for buildings with CBF. (**) Lateral torsional buckling of beams is prevented by RC-floor (no composite action).

	Type	Reference code	Criteria
A	Dynamic instability (Global)	-	Limit
B	Maximum roof drift ratio (Global)	FEMA 356	Indicative
C	Inter-story drift ratio (Global)	FEMA 356	Indicative
N	Ultimate rotation of link (Local)	FEMA 356	Limit
E	Shear capacity (Local)	EN1993-1	Limit
G	Global buckling (Local)	EN1993-1	Limit
H	Joints forces	-	Evaluation
I	Foundation forces	-	Evaluation

Table 9: Failure criteria for buildings with EBF.

4.2 Pushover analysis

In push-over (PO) analysis the non-linear behaviour, the relevant collapse criteria and the available q-factor of each structure were evaluated. Pushover analyses were performed on each structure using a monotonically increasing triangular pattern of lateral loads, applying, at the same time, the vertical loads ($G+0.3Q$), being G the sum of the self weight and the slab weight and Q the live load. The lateral loads were applied monotonically in a step-by-step nonlinear static analysis, as simply represented in the figure 7 in the case of building 2.

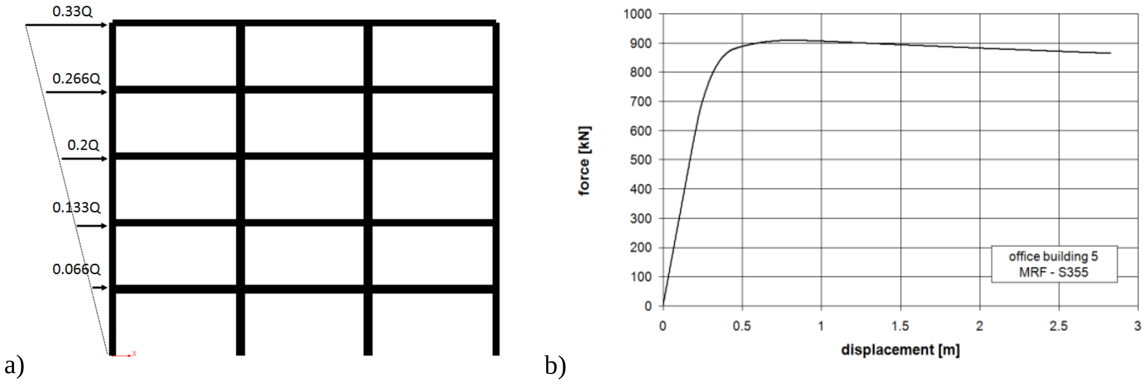

Figure 8: a) Pushover analysis in Abaqus for 2D MRF (X-direction) of Office Building 5, b) Diagram Q versus δ, for pushover analysis in Abaqus, for MRF and S355

The behaviour factor was determined on the basis of the base shear-displacement curve using the following formula:

$$q_{stat} = \frac{d_u}{d_y} \cdot \frac{V_y}{V_u}, \tag{10}$$

where d_y is the displacement at the first plastic hinge, V_y the corresponding base shear, d_u the displacement when the first failure criteria is reached and V_u the corresponding base shear [26].

4.3 Incremental dynamic analysis

In the second step the structures were analyzed by Incremental Dynamic Analysis (IDA), using the original accelerograms multiplied for a gradually increasing factor until the collapse of the structure was reached. According to EN1998-1-1 [1] prescriptions, seven earthquake time-histories of natural or artificially generated earthquakes can be used for the analyses. In order to obtain representative results for any seismic area in Europe, artificial accelerograms meeting the elastic response spectra presented in EN 1998-1 and consistent with chosen hazard model were adopted for numerical simulations. The program SIMQKE, developed by Gasparini and Vanmarcke [20] was used for the artificial generation of time histories.

Two types of seismic intensities were considered: for high seismicity areas the PGA level was equal to 0.25 g and the type 1 spectrum for soil category B was used; for low seismicity areas, on the other hand, the PGA was fixed to 0.10 g and the type 2 spectrum for soil type C was applied (figure 8a). The filter function was defined by a trapezoidal shape, where the time intervals for the initial and ending ramps were equal to 5.0 s and the strong motion duration was 10 or 5 s respectively for high and low seismicity (figure 8b). The relevant Eigen-periods were assumed to be in a range between 0.1 s and 3.0 s. The chosen sampling interval of Δt = 0.01 s allowed a sufficient accurate calculation for Eigen-frequencies up to 20 Hz (5 points for each period).

The verification of the accelerograms by determining the velocity and displacement time histories showed that the displacements were running out (figure 9), evidencing the necessity of the application of a baseline correction in order to obtain a sufficient small displacement at the end of the record. The adequacy of the accelerograms was checked by determination of their elastic response spectra (figure 10): for periods lower than T_B the spectral acceleration S_a was slightly too high (figure 11). Anyway, the target spectrum was sufficiently met and the requirements defined in EN1998-1 [1] were pursued.

The COV of the spectral values for the 7 accelerograms varied between 0.04 and 0.12 (figure 12). It should be noted that the energy density of artificial accelerograms is generally higher than the one of natural accelerograms, since all interesting frequencies are included.

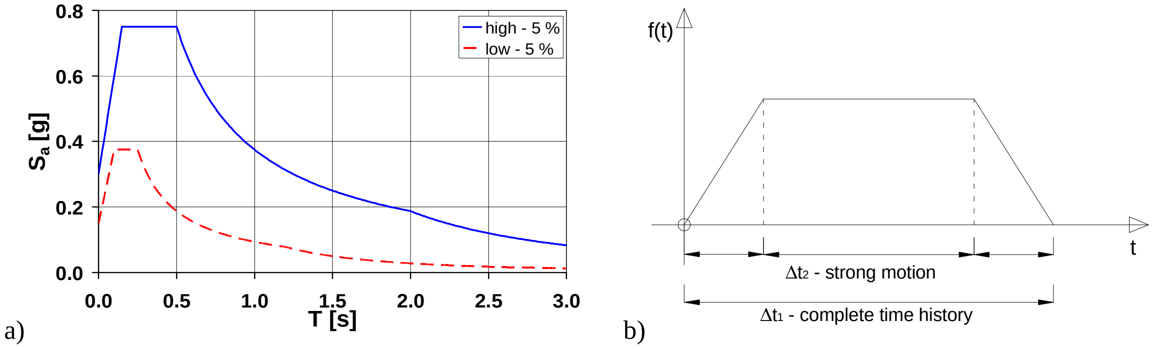

Figure 9: Target spectra (a) and filter function (b) for the generation of artificial time histories

Seismicity	PGA	Spectrum	Soil	Total duration	Strong motion duration
Low	0.10 g	Type 2	Type C	15 s	5 s
High	0.25 g	Type 1	Type B	20 s	10 s

Table 10: Parameters of target spectra and filter function for low and high seismicity

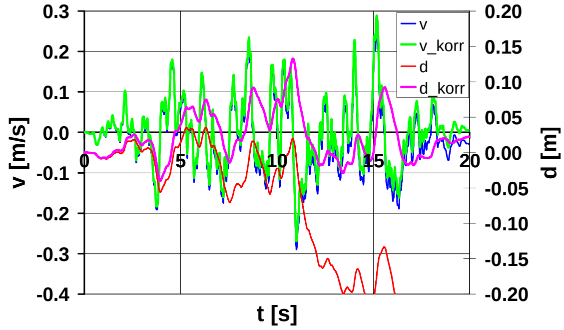

Figure 10: Baseline correction for an artificial accelerogram (high seismicity)

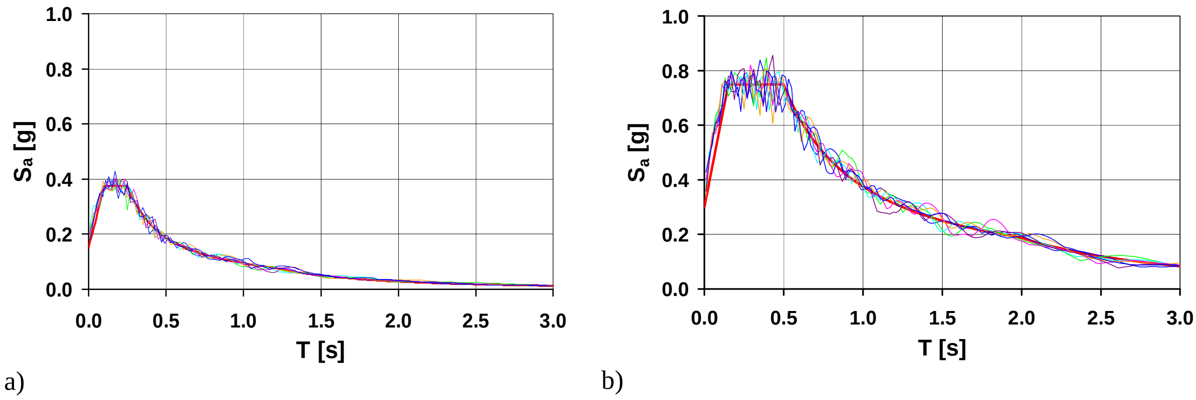

Figure 11: Target spectrum and elastic response spectra of 7 artificial accelerograms: a) low seismicity and b) high seismicity.

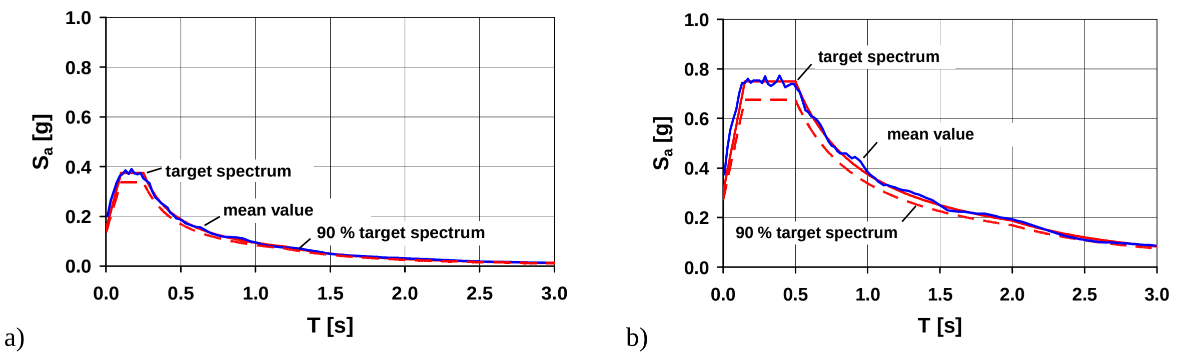

Figure 12: Target spectrum and mean value of the elastic response spectra of 7 artificial accelerograms: a) low and b) high seismicity

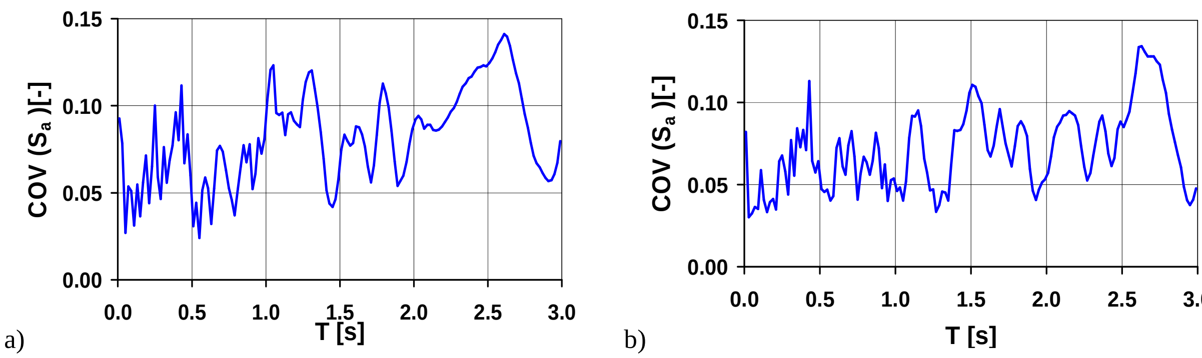

Figure 13: COV of the elastic response spectra of 7 artificial accelerograms: a) low and b) high seismicity.

Once identified the PGA able to activate relevant collapse modes, a modified Ballio-Setti procedure was used to determine the behaviour factor (q). The Ballio-Setti procedure was slightly modified for taking into account the discrepancy at first mode frequency between the target spectra and real spectra of earthquake time-histories (figure 13).

The available q-factors evaluated on the basis of IDAs' results were determined according to equation (11):

$$q = \frac{\lambda_u}{\lambda_{e,static}} \cdot \frac{a_{s,art}}{a_{sd}} \tag{11}$$

where λ_u is the accelerogram multiplier at the first limit state, $\lambda_{e,static}$ is the equivalent static seismic forces' multiplier corresponding to the first attainment of the plastic hinge in an elastic geometrically non linear pushover analysis, $a_{s,art}$ is the acceleration of the spectrum of the current accelerogram and a_{sd} the acceleration of the design spectrum, both corresponding to the fundamental period of the structure.

In the classic Ballio-Setti approach [12, 13], the second term, defined by the ratio between design spectrum PGA and artificial earthquake spectrum PGA, was not considered and the discrepancy between two PGA levels could strongly influence seismic behaviour assessment and the evaluation of the behaviour factor.

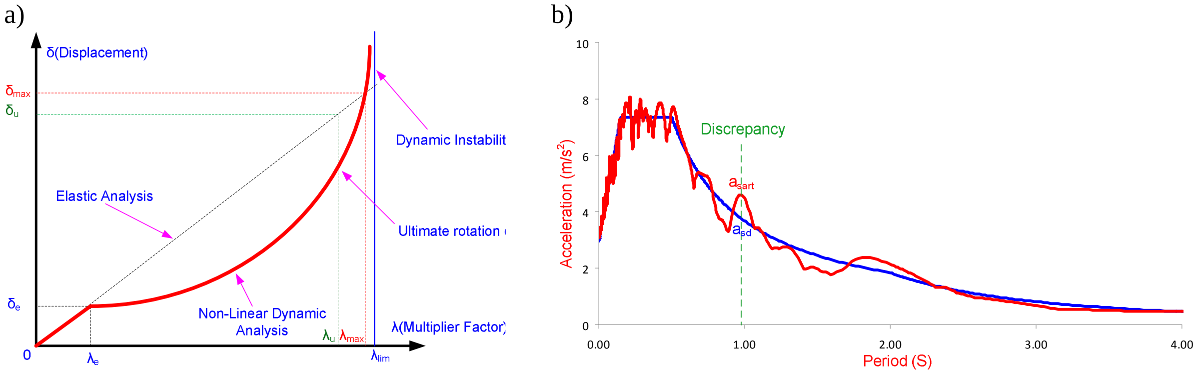

Figure 14: a) Scheme of the Ballio-Setti procedure, b) discrepancy between target spectrum and real spectrum.

4.4 Analysis of results and evaluation of q-factor

In the following paragraph, the evaluation of behaviour factors is presented considering buildings in relation to their structural typology, as well as described in the tables 3, 4 and 5.

Buildings n°1, 2, 14 and 15

The results of numerical simulations evidenced that MRF structures resisted PGA levels higher than the ones adopted in the initial design process executed using the lateral force method (table 9) The high resistance of those structures was related to the fact that seismic design requirements leaded to a general overstrength of the structure, compared to the resistance effectively required for the applied seismic design loads. Such effects were more considerable in the case of structures designed for moderate seismic actions (buildings n°1, 2 and 14), since the seismic design requirements were applied to ensure a sufficient performance of structures not only for low but also for high seismic actions characterized by longer strong motion periods.

In the MRF structures the ultimate rotation ratio was the controlling failure criterion. In the offices, as well as in the industrial buildings, the columns were the critical elements, whose ultimate rotation capacity was often reduced as a consequence of the applied axial loads. The scattering of the ultimate rotation ratio between accelerograms was considerably high (80 – 140 % and 80 – 130 %); the other failure criteria were not dominant, except for the interstorey drift ratio.

In the buildings characterized by CBF structure, the ultimate deformation of the bracings in compression was the governing failure criterion, but this criterion was neglected (since directly considered in the non linear models) and the investigations were focused on the deformation in tension criterion. The capacity ratios of the other failure criteria were rather low; the scattering of the results between different accelerograms was lower than the one evaluated for the MRFs, especially in the case of industrial buildings.

The values obtained for the behaviour factor using static non linear analysis are presented in table 11, while table 12 presents the values coming from the adoption of IDAs.

Building	1-xdir	2-xdir	14-xdir	15-xdir	15-ydir
d_y [m]	0,12	0,11	0,37	0,11	0,13
d_u [m]	0,28	0,27	0,96	0,40	0,28
V_y [kN]	709	1295	800	862	1204
V_u [kN]	830	1332	816	1164	1255
q	1,96	2,36	2,55	2,81	2,07

Table 11: Behaviour factors of case study 1, 2, 14 and 15 based on a non-linear static analysis.

Building	1-xdir	2-xdir	14-xdir	15-xdir	15-ydir
$\lambda_{e,static}$	1,54	1,28	1,32	1,27	0,85
λ_u	9,84	6,88	6,04	8,44	7,66
a_{sd} [g]*	0,07	0,046	0,477	0,034	0,055
$a_{s,art}$ [g]*	0,072	0,046	0,335	0,037	0,057
q**	6,66	5,37	3,24	7,04	9,23

Table 12: Limit states of steel structures with moment-resisting (MRF) and concentrically braced frames (CBF). (*) mean value of 7 accelerograms; (**) mean value of q-factors determined individually for 7 accelerograms.

Building n°10

As already presented, structures were assessed following the modified Ballio-Setti method, according to the improvement previously proposed. Results are presented considering the building as designed both in low and in high seismicity (design PGA respectively equal to 0.10 and 0.25g). IDA curves corresponding to EBF frame in high seismicity (PGA 0.25g, redesigned building n°10) are presented in figure 14b in terms of maximum displacement versus acceleration multiplier considering the 7 different artificial accelerograms, while figure 14a presents the same results expressed in terms of maximum base shear versus maximum top displacement. In general, due to the rather stiff behaviour of the braced structure, non linear geometrical effects did not lead to the dynamic instability of the structure, and the non linear behaviour was essentially governed by material non linearities. This situation was observed for all the four bi-dimensional frames studied, although less pronounced for CBF frame in high seismicity. The values of the behaviour factor based strictly on the modified Ballio-Setti method previously described are presented in table 13 for the cases where an intersection is identified.

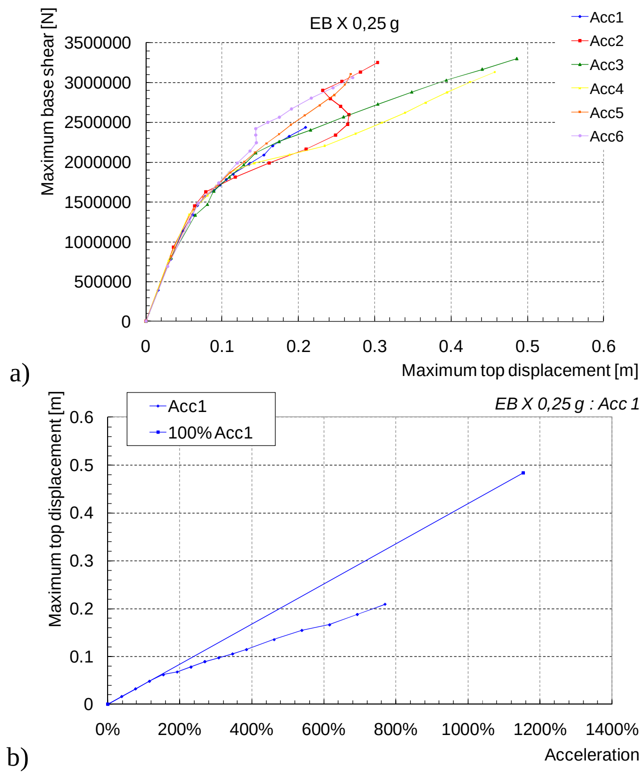

Figure 15: a) IDA curves for EBF, b) PO curve in term of maximum displacement vs acceleration multiplier for accelerogram n°1 (EBF building n°10, x direction).

Building n°10	Behaviour factor						
	Acc. 1	Acc. 2	Acc. 3	Acc. 4	Acc. 5	Acc. 6	Acc. 7
EB X 0,10 g	7,5	--	--	--	--	--	--
CB Y 0,10 g	--	--	--	--	--	--	--
EB X 0,25 g	--	5	--	6,5	--	--	--
CB Y 0,25 g	--	6,5	--	2	--	2,75	3

Table 13: Behavior factors based on IDA curves.

The values of the behaviour factor so obtained were very high (table 14), as a consequence of the fact that the presented evaluations were based on the assumption of an infinite deformation capacity of the structure. It is thus necessary to check to what extent the structural ductility can effectively be used. For EBF/CBF composite structures, the premature failure was triggered by an excessive demand on the ductile zones: i.e. excessive rotation of links for EBFs and excessive axial deformation of braces for CBFs, with limit values assumed in agreement to FEMA 356 prescriptions.

Accelerogram	q- factor for CBFs				q- factor for EBFs			
	PGA 0.1g		PGA 0.25g		PGA 0.1g		PGA 0.25g	
	SL	CP	SL	CP	SL	CP	SL	CP
1	4.6	--	--	--	7.5	7.5	5.4	6.9
2	5.4	--	6.2	6.5	--	--	3.5	3.8
3	6.2	--	--	--	--	--	6.2	6.9
4	5.4	--	2.0	2.0	--	--	4.6	4.6
5	6.2	--	--	--	--	--	6.2	--
6	5.4	--	2.75	2.75	--	--	--	8.5
7	6.2	--	3.0	3.0	--	--	5.4	6.9
Mean Values	*5.6*	*-- (*)*	*3.5*	*3.6*	*7.5 (**)*	*7.5 (**)*	*5.2*	*5.8*

Table 14: Behaviour factors. (*) CP level of the criterion is never reach by any of the 7 accelerograms even for a multiplier equal to 15; (**) Only one out of the 7 ground motion time-history is able to trigger the collapse criterion. For all other six, collapse is not reach even for an accelerogram multiplier equal to 15.

According to what presented in the table 14, EBFs were characterized by values of the allowable q-factor higher than the ones adopted in the design, also in the case of CP limit state. In the particular case of an EBF designed for low seismicity, the homogeneity rules on the over-strength factor of the joints provided an inherent global over-strength of the building, leading to q-factors higher than 7.5.

Regarding CBFs, results strongly varied if the limit state was considered as governed by compression or tension collapse of the diagonal. If the limit state was assumed to be governed by the compression limit, the behaviour factors obtained in average for the seven accelerograms were in the range between 1.7 and 3.3.

A deeper insight in the analysis of results showed that the rather poor ductility of the system obtained under these assumptions was related to a deformation concentration at the top storey of the building, due to the high slenderness of the diagonal. In the design of presented case studies, the upper limit on the diagonal slenderness was released for the 2 upper levels due the quasi-impossibility to fulfil simultaneously all the design criteria and arguing that according to Eurocode 8, the limit was not mandatory for 2-storeys building: if the potential collapse of the 5th storey was assumed to be governed by tension only, results became, on the other hand, very close to the ones obtained considering tension only at all levels. Under this assumption, allowable q-factors became higher than the ones considered in the design for low-seismicity conditions and slightly lower for high-seismicity.

Buildings n° 6, 7, 8 and 9

Building n° 6 was designed for low seismicity hazard and presented bare steel columns (table 5). The most conditioning criteria in the assessment of the building were related to beams' and columns' ductility and to the intensity of applied axial loads.

The q factor evaluated according to what previously presented was around 7 using the modified Ballio-Setti method, and around 8 using the classic method; the design behaviour factor, on the other hand, was equal to 4 [1]. As a consequence, the adoption of Medium Ductility Class (DCM) behaviour in low seismicity areas provided structural solutions not completely optimized, in which the structural capacity, in terms of q factor, was twice the design values (table 15).

Despite the high values of obtained q-factors for low seismicity, it's important to underline that, in these cases, the design was not guided by seismic action but by wind action: as a consequence, overstrength criteria to ensure the weak beam-strong column condition made the structure overdesigned.

Building n° 7 was designed for high seismicity hazard and presented partially encased composite columns (table 5); the design was executed assuming a design q factor equal to 4 for DCM behaviour. The estimated q factor was around 8.5 adopting the classical procedure and around 8 using the modified Ballio-Setti method (table 15), evidencing, also in this case, a significative overstrengthening of the elements' size.

Building n° 8 was designed for high seismicity using bare steel columns; in this case, the significant collapse criteria were related to the reaching of the ultimate rotation of plastic hinges located at the ends of beams and at the base of columns. The values of ultimate rotations were fixed according to the limit values indicated by FEMA356 [19].

The minimal rotation capacity, equal to 20 mrad according to Eurocode 8, leaded to values of the allowable ductility in terms of q-factor equal to 2.5 or 2.6 respectively adopting the modified and the classical method, differently from what imposed in the design process (behaviour factor equal to 4.0).

The values of the evaluated behaviour factors for selected case studies are presented in the table 15: as visible, in high seismic hazard q factor obtained from numerical analyses were lower than the ones adopted in the design (i.e. assuming DCM condition). On the contrary for the structures designed with a low seismic hazard, the q factor obtained from numerical simulations was systematically higher (at least 2 times) than the values adopted for the design.

Building	Modified Ballio-Setti method	Classic method	Design q factor
6	7.0	8.0	4.0
7	8.0	8.5	4.0
8	3.0	3.75	4.0
9	Not evaluated	Not evaluated	4.0

Table 15: q factor of the different buildings calculated using different methods.

Buildings n° 5, 12 and 13

Buildings n° 5, 12 and 13 (respectively, five-storey office building, four-storey industrial building and single-storey industrial building) were designed adopting two different steel grades qualities for each building considering a design PGA equal to 0.25 g.

The collapse criteria assumed for the execution of IDAs were the ones defined by FEMA356 [19], EN1993 [16] and EN1998 [1, 18]. IDAs were executed considering the 7 artificial accelerograms: original accelerograms were multiplied by factors varying between 0.5 and 20, in order to individuate the significant collapse criteria for each structural typology. As example, in the figure 16 the results coming from IDA simulations were gathered in order to trace IDA curves and to individuate the PGA levels corresponding to collapse criteria activation. The values of q-factors coming from PO (q_{PO}) and IDA (q_{IDA}) are presented in the table 16: as visible, a strong variability was revealed considering the two different methods of analysis. In general, the results of PO analyses leaded to lower values of behaviour factors, especially if compared to the ones provided by IDAs' results: for example in the case of building n°5 (y direction) q-factors varied between 3.11 and 6.28 (steel grade S355), or in the case of building n°12 (x direction) between 1.71 and 9.97 (steel grade S355).

Building n°	5 (S355 X)	5 (S460 X)	5 (S355 Y)	5 (S460 Y)	12 (S355 X)	12 (S460 X)
q_{PO}	1.98	1.98	3.11	2.55	1.71	1.63
q_{IDA}	2.80	2.68	6.28	6.04	9.97	9.56
Building	12 (S355 Y)	12 (S460 Y)	13 (S235 X)	13 (S275 X)	13 (S235 Y)	13 (S275Y)
q_{PO}	2.33	1.63	2.02	2.13	4.05	3.87
q_{IDA}	2.54	2.31	3.74	2.83	6.45	5.98

Table 16: Results for q-factor using pushover analysis and IDA.

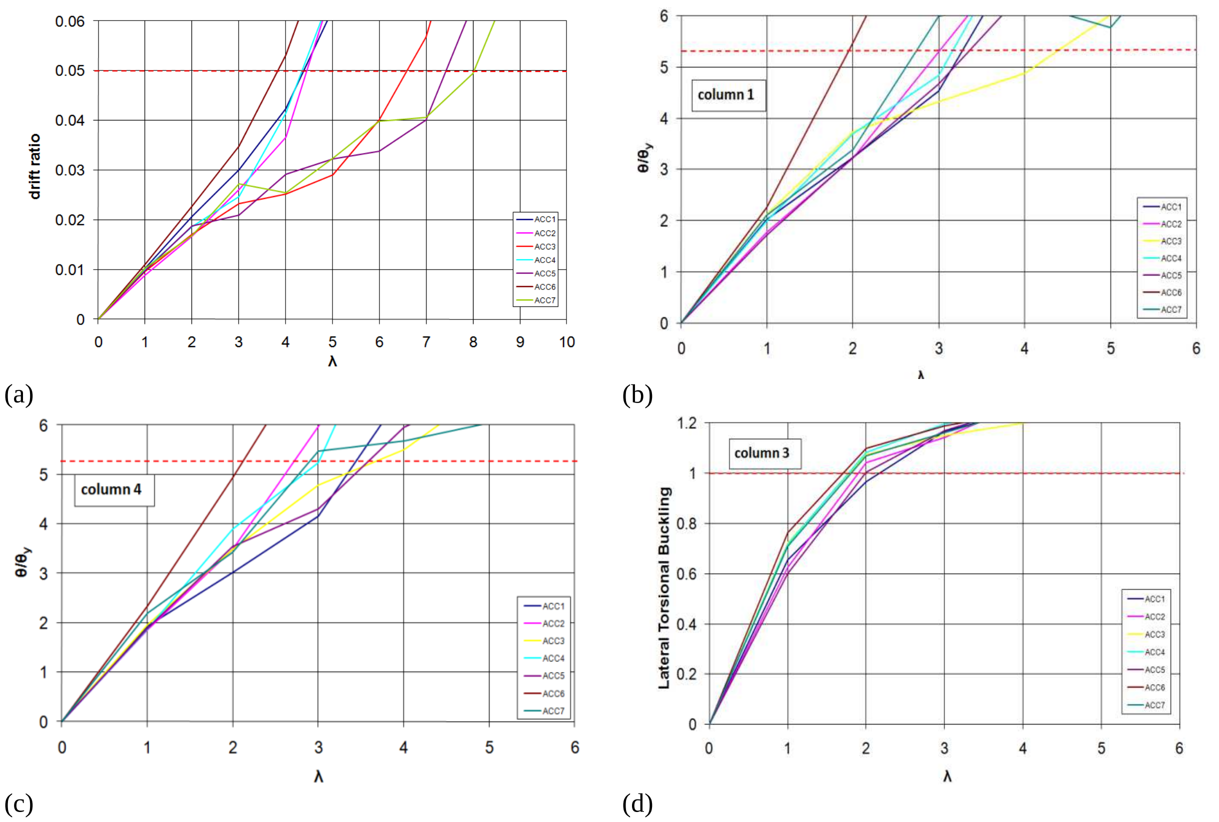

Figure 16: IDA curves for different time-histories and individuation of collapse levels: (a) drift ratio; (b) ultimate plastic hinge rotation; (c) ultimate plastic hinge rotation; (d) column buckling.

Buildings n° 3, 4 and 16

Buildings were designed considering the adoption of High Ductility Class (DCH) in high seismicity (design PGA 0.25g) for buildings n°3 and n°16, using shear link, and DCM in low seismicity for building 4 (design PGA 0.15g). The design behavior factor were equal to 6 (buildings 3 and 16) and 4 (building 4), while PO and IDAs were adopted for the evaluation of the effective allowable ductility.

Frames in medium – low seismicity area (frames 4x and 4y, table 18) were characterized by very low values of the effective q-factor, especially if the Modified Ballio – Setti method was considered; on the other hand, taking into account the traditional evaluation of q-factor, the difference between the numerical and the design behaviour factor became smaller, leading to values very close to the design one (i.e. frame 4x). This fact was mainly due to the factor $a_{s,art}/a_{s,d}$: the local difference between the accelerogram and the spectrum was higher than 5% (medium value considered by Eurocode for the definition of spectrum compatibility).

The execution of all numerical simulations clearly showed the impossibility of activating the collapse criteria related to columns; at the same time, in the case of braces (buckling of members in compression) the equivalent q factors were so high to make the exploration of the corresponding PGA level without technical meaning. PGA activation levels were determined for each relevant collapse criteria; moreover, preliminary IDA pilot simulations were carried out considering the real mechanical properties values (i.e. mean values of production data) and evaluating the following modification of activation PGA for the selected collapse criteria.

Such pilot simulations evidenced that the insertion of real mechanical properties moved PGA level to activate bracing collapse, neglecting, once again, columns' criteria.

Acc n°	q- factor for 3 EBF X				q- factor for 3 EBF Y			
	Link	Column	Brace	Drift	Link	Column	Brace	Drift
1	11,80	Not sig.	Not sig.	7,90	8,30	Not sig.	13,80	9,20
2	9,30	Not sig.	Not sig.	9,30	8,30	Not sig.	11,60	9,10
3	9,80	Not sig.	Not sig.	11,80	8,50	Not sig.	11,00	9,30
4	7,40	Not sig.	Not sig.	7,40	7,00	Not sig.	10,10	7,70
5	10,90	Not sig.	Not sig.	7,90	6,60	Not sig.	9,90	6,60
6	7,00	Not sig.	Not sig.	7,70	9,50	Not sig.	11,20	10,30
7	9,10	Not sig.	Not sig.	10,90	8,80	Not sig.	11,20	8,80

Table 17: q factor estimation using IDA simulations – Building 3.

Acc n°	q- factor for 4 EBF X				q- factor for 4 EBF Y			
	Link	Column	Brace	Drift	Link	Column	Brace	Drift
1	2,57	12,90	3,90	5,80	2,60	13,10	13,10	7,80
2	2,27	9,10	3,60	6,40	2,70	10,80	10,80	4,90
3	2,71	10,80	3,30	5,40	2,40	9,70	9,20	4,60
4	2,13	9,50	2,40	4,50	2,70	11,80	9,50	4,20
5	2,67	10,70	3,20	5,90	1,90	10,90	10,90	6,30
6	2,40	10,60	2,70	6,40	2,20	11,10	10,60	4,40
7	2,34	9,40	2,60	5,60	2,90	11,60	11,60	7,00

Table 18: q factor estimation using IDA simulations – Building 4.

Acc n°	q- factor for 16 EBF X				q- factor for 16 EBF Y			
	Link	Column	Brace	Drift	Link	Column	Brace	Drift
1	12,00	Not sig.	11,00	13,90	15,30	Not sig.	18,50	17,40
2	12,00	Not sig.	11,00	13,90	12,30	Not sig.	15,00	13,20
3	12,70	Not sig.	11,60	14,80	11,20	Not sig.	16,00	12,80
4	9,90	Not sig.	9,90	10,90	9,60	Not sig.	13,10	12,30
5	11,80	Not sig.	9,90	12,80	10,30	Not sig.	12,90	12,90
6	10,40	Not sig.	10,40	12,20	9,40	Not sig.	12,80	12,80
7	12,70	Not sig.	10,90	14,50	12,40	Not sig.	17,70	14,20

Table 19: q factor estimation using IDA simulations – Building 16.

5 COMPARISON AND CONCLUSIONS

Table 20 briefly summarizes what already presented as regards the q-factor values obtained from pushover and IDA analyses with respect to the values adopted in the design according to actual standards and to what specified in the previous paragraphs.

As visible, in the majority of cases for both the two considered main directions of the designed buildings, the values of the q-factor obtained using IDAs were higher than the ones adopted in the design, evidencing a substantial overstrength of buildings designed in high seismicity areas.

Looking at the results presented in table 20, buildings realized in low seismicity areas (characterized by a design PGA equal to 0.10g like buildings 1, 2, 6, 7, 10 and 15) were associated to higher values of the behaviour factor (evaluated adopting IDA procedure) respect to the ones adopted during the design process, leading consequently to the oversizing of structural members. As an example, in the case of building n°1, the q-factor adopted in the design was equal to 3.99 while the one obtained from the evaluation using IDA was equal to 6.66. A similar condition was revealed also for building n°2 (frame in x direction) with design value of 4.00 towards an evaluated one up to 5.37, and in the case of building n°7 with design value 4.00 versus an obtained q_{IDA} equal to 7.00.

On the other hand, considering the case of EBF structure with long bending link (building n°4) the behaviour factor evaluated according to EN 1998-1:2005 [1] seems to be over-estimated, with assumed values in the design process equal to 4.00 for both the two main directions of the building and obtained values from IDAs respectively equal to 2.45 and 2.48 for x and y directions. Otherwise, considering the structural behaviour of buildings designed for high seismicity (PGA equal to 0.25g), the q-factors assumed in the design are generally lower (or at least equal) than the ones evaluated using the modified Ballio-Setti method before presented, evidencing the correct approach of EN1998-1:2005 for the design.

Finally, table 20 presents the results obtained from buildings (indicated by the adoption of the asterisk) that were re-designed using lower q-factor values according to a preliminary evaluation using the presented Ballio-Setti procedure. In this sense, the above mentioned procedure can be used in order to optimize the design of structures.

N°	X – direction			Y – direction			q Design		PGA
	system	q_{static}	q_{IDA}	system	q_{static}	q_{IDA}	x	y	[g]
1	MRF	1,96$^{(**)}$	6,66	Not des.	-	-	2,35	3,99	0,10
2	CBF	2,36$^{(**)}$	5,37	Not des.	-	-	3,68	4,00	0,10
3	EBF shear	5,78	8,32	EBF shear	7,66	8,11	6,00	6,00	0,25

4	EBF bending		3,18	2,45	EBF bending		3,90	2,48	4,00	4,00	0,15
5	MRF	S355	1,98	2,80	CBF	S355	3,11	6,28	4,00	4,00	0,25
		S460	1,98	2,68		S460	2,55	6,04			
6	MRF		2,65(**)	7,00	Not des.		-	-	4,00	4,00	0,10
7	MRF		2,60(**)	8,00	Not des.		-	-	4,00	4,00	0,10
8	MRF		1,80(**)	3,00	Not des.		-	-	4,00	4,00	0,25
9	MRF		1,75(**)	-	Not des.		-	-	4,00	4,00	0,25
10	EBF vertical shear link		6,78	7,50(*)	CBF		4,30	5,60	4,00	4,00	0,10
11	EBF vertical shear link		6,62	5,20	CBF		4,00	3,50	4,00	4,00	0,25
12	MRF	S355	1,71	9,97	CBF	S355	2,33	2,54	4,00	4,00	0,25
		S460	1,63	9,56		S460	1,63	2,31			
13	MRF	S235	2,02	3,74	CBF	S235	4,05	6,45	4,00	4,00	0,25
		S275	2,13	2,83		S275	3,87	5,98			
14	MRF truss girder		2,55	3,24	CBF		-	-	1,55	3,80	0,25
15	MRF		11,5	12,32	CBF		4,66	7,47	1,96	2,64	0,10
16	EBF shear		2,81	7,04	EBF (shear)		2,07	9,23	6,00	6,00	0,25

Table 20: Summarizing table of q factors obtained from pushover and IDA with respect to design values. (*) frames re-designed lower q factor - values under re-evaluation (**) no material over-strength ($V_{y,real}/V_{y,design}$)

Acknowledgements The present work was developed inside the European Research Project OPUS (RFSR-CT-2007-00039), funded by the Research Fund for Coal and Steel (RFCS). It was also part of the Italian research project RELUIS, funded by Italian Department for Civil Protection.

REFERENCES

[1] UNI-EN1998-1-1: Eurocode 8 - Design of structures for earthquake resistance. Part 1: General rules, seismic actions and rules for buildings. Technical Commission 250/SC8, Brussels, 2005.

[2] ICBO – International Conference of Building Officials, (1997). Uniform building code – vol.2: structural engineering design provisions. California: Whittier.

[3] FEMA, (1995). NEHRP recommended provisions for seimsic regulations for new buildings, part I – provisions; part 2 – commentary. Washington DC: BSSC.

[4] AISC – American Institute of Steel Construction (2005). Seismic Provisions for Structural Steel Buildings. ANSI/AISC 341-05, AISC INC. Chicago, Illinois.

[5] A.Y. Elghazouli, Assessment of European seismic design procedures for steel framed structures. *Bullettin of Earthquake Engineering*, **8**(1), 65-89, 2010.

[6] M. Bosco, P.P. Rossi, Seismic behaviour of eccentrically braced frames. *Engineering Structures*, **31**, 664-674, 2009.

[7] EN10025-1÷6 General technical delivery conditions for: non-alloy, normalized/normalized rolled weldable fine grain, thermomechanical rolled weldable fine grain, improved atmospheric corrosion resistance, flat products of high yield strength in the quenched and tempered condition. European Committee for Standardization, Brussels, 2004.

[8] A. Longo, R. Montuori, V. Piluso, Influence of Design Criteria on the Seismic Reliability of X-braced Frames. *Journal of Earthquake Engineering*, **12**(3), 406- 431, 2008.
[9] P.P. Rossi, A. Lombardo, Influence of the link overstrength factor on the seismic behaviour of eccentrically braced frames. *Journal of Constructional Steel Research*, **63**, 1529–1545, 2007.
[10] AA.VV., (2011). Optimizing the seismic Performance of steel and steel-composite concrete strUctures by Standardizing material quality control, Research Fund for Coal and Steel, contract RFCR-CT-2007-00039, final report, Technical Steel Research Series, European Commission.
[11] M. Badalassi, A. Braconi, S. Caprili, W. Salvatore, Influence of steel mechanical properties on EBF seismic behaviour. *Bulletin of Earthquake Engineering*, under review, 2013.
[12] G. Ballio, F. Perotti, L. Rampazzo, P. Setti, Determinazione del fattore di struttura per costruzioni metalliche soggette a carichi assiali. *II Convegno nazionale ANIDIS, L'ingegneria Sismica in Italia*, Rapallo, 1984.
[13] P. Setti, Un metodo per la determinazione del coefficiente di struttura per le costruzioni metalliche in zona sismica. *Costruzioni Metalliche*, **3**, 1985.
[14] UNI-EN1991-1-1: Eurocode 1 – Actions on structures. Part 1-1: General actions - Densities, self-weight, imposed loads for buildings, Technical Commission 250, Brussels, 2005.
[15] UNI-EN1990: Eurocode Basis of structural design. Technical Commission 250, Brussels, 2005.
[16] UNI-EN1993-1-1: Eurocode 3 – Design of steel structures. Part 1-1: General rules and rules for buildings. Technical Commission 250/SC3, Brussels.
[17] UNI-EN1994-1-1: Eurocode 4 – Design of composite steel and concrete structures. Part 1-1: General rules and rules for buildings. Technical Commission 250/SC4, Brussels.
[18] UNI-EN1998-3: Eurocode 8: Design of structures for earthquake resistance - Part 3: Assessment and retrofitting of buildings, 2005.
[19] FEMA 356, ASCE - Prestandard and commentary for the seismic rehabilitation of buildings, 2000.
[20] E.H. Vanmarcke EH, G.A. Gordon, E. Heredia-Zavoni, SIMQKE-II, conditioned earthquake ground motion simulator: user's manual, version 2.1, Princeton University, U.S.A, 1999.
[21] Abaqus, Users' manual. Hibbitt, Karlsson, and Sorensen, Inc., 2005.
[22] FineLg User's Manual, V9.2. Greisch Info – Department ArGEnCo – ULg, 2003.
[23] J. Kuck, B. Hoffmeister, User manual for DYNACS - A Program for DYnamic Nonlinear Analysis of Composite and Steel structures (unpublished), 1993.
[24] S. Mazzoni, F. McKenna, M.H. Scott et al., Opensees command Language Manual, 2007.
[25] M. Menegotto, P. Pinto, Method of analysis for cyclically loaded reinforced concrete plane frame including changes of geometry and non elastic behavior of elements under combined normal force and bending, *IABSE Symposium on resistance and ultimate deformability of structures acted on by well defined repeated loads*, Lisbon, 1973.
[26] M. Bruneau, C. Uang, A. Whittaker A., Ductile design of steel structures, McGraw Hill, 1998.